

Species occurrence as a function of both emergent biological traits
and environmental context

Peter D. Smits^{1,*}

1. University of Chicago, Chicago, Illinois 60637.

* Corresponding author; e-mail: psmits@uchicago.edu.

Manuscript elements:

Keywords:

Manuscript type: Article

Prepared using the suggested L^AT_EX template for *Am. Nat.*

Introduction

- 2 How do species pools change over time as species are recruited or go extinct? When are ecotypes
enriched or depleted? How does global and regional environmental context affect the distribution of
4 species ecotypes (e.g. guilds) in a regional species pool?

A regional species pool is the set of species which form communities in a specific region; local
6 communities are subsets of the regional pool. The composition of a regional species pool changes
over time due to speciation, migration, extinction. Local scale processes like resource competition
8 only affect the regional species pool if all communities are affected.

Valentine and Bambach how they presented guilds in paleobiology which is taxa united by
10 similarity of their macroecology (Bambach, 1977; Valentine, 1969). Bush and Bambach presented
an ecocube to describe what how marine invertebrates partition space and resources (Bambach
12 et al., 2007; Bush and Bambach, 2011; Bush et al., 2007). Unique combinations represent what
possible ecotypes are observable. The distribution of ecocube occupancy is then normally analyzed
14 as raw counts of unique combinations or using ordination methods and the change in disparity over
time is estimated (Bambach et al., 2007; Bush and Bambach, 2011; Bush et al., 2007).

16 Analysis of mammal diversity and hypotheses as to the processes that have shaped it tend to fall
under a few categories: diversity of the whole system (Alroy, 1996; Alroy et al., 2000; Figueirido
18 et al., 2012; Liow et al., 2008), guild based (Janis et al., 2004; Janis, 2008; Janis et al., 2000; Janis
and Wilhelm, 1993; Jernvall and Fortelius, 2004; Pires et al., 2015), clade based (Quental and
20 Marshall, 2013; Silvestro et al., 2015; Slater, 2015), climate based (Blois and Hadly, 2009; Janis,
1993; Janis and Wilhelm, 1993), and location based (Badgley and Finarelli, 2013; Eronen et al.,
22 2015). Rarely are more than two of these categories considered simultaneously, and instead
integration of these diverse observations and hypotheses tends to be based on coincidence. The goal
24 of this study is to pool information from multiple levels of organization by integrating both species
and climate data into a single analysis in order to provide a more holistic interpretation of the
26 processes which may have shaped mammal species diversity.

Fourth-corner modeling is an approach to explaining the patterns of either species abundance or
28 presence/absence as a product of species traits, environmental factors, and the interaction between
traits and environment (Brown et al., 2014; Jamil et al., 2013; Pollock et al., 2012; Warton et al.,
30 2015) CITATION. In modern ecological studies, what is being modeled is species occurrences at
localities distributed across a region (Jamil et al., 2013; Pollock et al., 2012). In this study, what is
32 being modeled is the pattern of species occurrence over time for most of the Cenozoic in North
America (Fig. 1). These two approaches, modern and paleontological, are different views of the same
34 three-dimensional pattern: species at localities over time. The temporal limitations of modern
ecological studies and difficulties with uneven spatial occurrences of fossils in paleontological studies
36 means that these approaches are complimentary but reveal different patterns of how species are
distributed in time and space.

38 One of the greatest challenges with analyzing species occurrence data is the inherent incompleteness
of any sample (Foote, 2001; Foote and Sepkoski, 1999; Lloyd et al., 2011; Royle and Dorazio, 2008;
40 Royle et al., 2014; Wang and Marshall, 2016). In the modern, only presences are certain as an
absence can be caused by both the species being truly absent or the species never having been
42 sampled (Royle and Dorazio, 2008; Royle et al., 2014). For paleontological data in the context of
this study, the incomplete preservation of fossil communities combined with the incomplete
44 sampling of what fossils there are means that the true times of origination or extinction may not be
observed (Foote, 2001; Foote and Sepkoski, 1999; Wang et al., 2016; Wang and Marshall, 2016).

46 In the analyses done here, a few key covariates which describe species' macroecology and
environmental context are considered. Because of the complexity of fourth-corner analyses in terms
48 of both number of covariates considered and structure of each model, it is possible to consider and
test a large number of possible hypotheses. Presented here are the species traits and related
50 hypotheses, followed by the environmental factors and related hypotheses.

The principle species trait considered in this study is a species' ecotype, defined here as the unique
52 combination of species dietary category and locomotor category (e.g. arboreal omnivore versus
unguligrade herbivore). This classification is analogous to the marine invertebrate ecocube discussed

54 above (Bush and Bambach, 2011; Bush et al., 2007; ?). Species mass was also included as a species trait, but is mostly included in order to control for that effect on species observation and occurrence.

56 Translating previous work into hypotheses applicable to this analysis is difficult. Taxonomic grouping is frequently invoked in many proposed hypotheses for how mammal diversity is structured (Janis, 2008; Janis and Wilhelm, 1993; Pires et al., 2015; Quental and Marshall, 2013; Slater, 2015). However, this practice is problematic because taxonomic grouping conflates shared evolutionary history and similarities in species macroecology which means that whatever aspects of species biology are important for the processes underlying species diversity are obscured.

62 Jernvall and Fortelius (2004) found that for the Neogene of Europe the relative abundance of mammal guilds was stable over time even in the face of high turnover rates.

64 Many discussions of the effects or associates of species ecology and diversity have focused on ungulate herbivores (Janis et al., 2004; Janis, 2008; Janis et al., 2000; Janis and Wilhelm, 1993) and 66 carnivores (Janis and Wilhelm, 1993; Pires et al., 2015; Silvestro et al., 2015; Slater, 2015).

The diversity history of ungulate herbivores is characterized by younger originating taxa having 68 longer legs, higher crowned teeth, and a preference for grazing over browsing than their earlier originating counterparts (Janis et al., 2004; Janis, 2008; Janis et al., 2000; Janis and Wilhelm, 70 1993); all of which have all been attributed to environmental change or tectonic activity driving climate and environmental change (Blois and Hadly, 2009; Eronen et al., 2015; Janis, 2008).

72 Additionally, it has been observed that ungulate cursorial forms arose before carnivore cursorial forms, an observation attributed to the reorganization of plant communities towards the end of the 74 Cenozoic (Janis and Wilhelm, 1993).

Within the canid guild of North America (e.g. plantigrade and digitigrade carnivores) there is 76 evidence that their diversity, or at least the structure of that diversity, is self-regulating in the sense that species from different clades are “competing” for niche or guild space in the North American 78 regional species pool (Silvestro et al., 2015).

A pattern of generally constant diversity through time is also observed within the canid carnivore

80 subguilds of hypercarnivore, hypocarnivore, and mesocarnivores though there was no evidence of
diversity-dependence in trait (e.g. body size) evolution (Slater, 2015). The general pattern of
82 constant diversity in the face of turnover is however consistent with a possibly self-regulating
system.

84 There is some uncertainty as to the effect of species body size on mammal diversity and aspects of
the diversification processes, specifically extinction (Liow et al., 2008, 2009; Smits, 2015; Tomiya,
86 2013).

88 Smits (2015) found several systematic differences in mammal species durations associated with
various species traits. Omnivorous taxa were found to have, on average, a greater duration than
other dietary categories. Additionally, arboreal taxa were found to have a shorter duration than
90 other locomotor categories.

92 An unresolved question from Smits (2015) is whether the greater extinction risk faced by arboreal is
constant over time or if there was a change in extinction risk at the Paleogene/Neogene boundary.
Specifically, the question is whether the extinction risk arboreal taxa increased in the Neogene,
94 driving the loss of arboreal taxa and average extinction risk of arboreal taxa down.

96 There are no observed massive cross-taxonomic turnover events in the North American record,
unlike the Neogene record Europe (Alroy, 1996, 2009; Alroy et al., 2000; Eronen et al., 2015; Janis,
1993).

98 Fundamentally, all species respond differently to climate and environmental change (Blois and
Hadly, 2009). Macroecological patterns are the similarities across species, the emergent properties
100 of how species react to a similar “stimulus.”

102 The Cenozoic is generally characterized by a global cooling trend and the development of polar
ice-caps during the Neogene, with a few notable exceptions (Cramer et al., 2011; Zachos et al., 2008,
2001). The Cenozoic of North America is additionally characterized by an environmental transition
104 from the closed, partially forested environments of the Paleogene to the savannah and grasslands
environments of the Neogene (Blois and Hadly, 2009; Janis, 1993; Janis et al., 2000; Strömborg,

¹⁰⁶ 2005).

With respect to North America specifically, much of regional climatic and environmental change has
¹⁰⁸ been attributed to tectonic activity and uplift (Badgley and Finarelli, 2013; Blois and Hadly, 2009;
Eronen et al., 2015; Janis, 2008) CITATIONS. Additionally, tectonic activity and uplift is
¹¹⁰ considered the driving causal mechanism behind both changes to diversity and trait evolution
(Badgley and Finarelli, 2013; Blois and Hadly, 2009) CITATIONS.

¹¹² The Eocene-Oligocene transition is associated with high extinction amongst ungulate taxa (Janis,
2008). This period is also the transition from the Paleogene to the Neogene and from herbivores
¹¹⁴ being browsing dominated to grazing dominated CITATION.

There is an observed stability in estimates of global temperature from the E/O transition till the
¹¹⁶ end of the Miocene; this is called the Mid-Miocene climatic optimum (Zachos et al., 2008, 2001).
The Mid-Miocene climatic optimum is bookended by periods of temperature decline.

¹¹⁸ The environmental factors included in this study include estimates of global tempreature and the
changing floral groups present in North America across the Cenozoic. These covariates were chosen
¹²⁰ because they provide high level characterizations of the environmental context of the entire North
American regional species pool for most of the Cenozoic. Importantly, the effects of a species
¹²² ecotype on diversity are themselves modeled as functions of environmental factors (Fig. 1) allowing
for inference as to how species ecology mediates environmental context.

¹²⁴ The effect of climate on diversity and the diversification process has been the focus of considerable
research with many analyses favoring diversification being more biologically-mediated than
¹²⁶ climate-mediated (Alroy, 1996; Alroy et al., 2000; Clyde and Gingerich, 1998; Figueirido et al.,
2012). Scale of analysis makes a big difference in interpretation of results, both temporal and
¹²⁸ geographic. For example when the mammal fossil record analyzed at small temporal and geographic
scales a correlation between diversity and climate are observable (Clyde and Gingerich, 1998).

¹³⁰ However, when the record is analyzed at the scale of the continent and the Cenozoic there is no
correlation with diversity and climate (Alroy et al., 2000). This results, however, does not go
¹³² against the idea that there may be short periods of correlation and that this correlation change or

reverse direction over time; instead this result means that there is no single direction of correlation
134 between diversity and climate (Figueirido et al., 2012).

In the case of a fluctuating correlation between diversity and climate it is hard to make the
136 argument of an actual causal link between the two without understanding the ecological differences
in mammalian fauna over time; when this analysis is based on diversity or taxonomy alone no
138 mechanisms are possible to infer. After all, taxonomy conflates many potential factors that could
affect diversification into a single variable; by separating the effects of shared common ancestry (i.e.
140 phylogeny) from species ecology the subtle differences in the diversification process can be observed
(Smits, 2015).

142 Ultimately, the goal of this analysis are to understand when are unique ecotypes enriched or
depleted in the North American mammal regional species pool and how changes in ecotypic
144 diversity are related to changes in species' environmental context.

Materials and Methods

146 Taxon occurrences and species-level information

All fossil occurrence information was downloaded from the Paleobiology Database.
148 Occurrences (PBDB) were restricted to all Mammalia sampled in North America between the
Maastrichtian and Gelasian stages. Taxonomic, stratigraphic, and ecological metadata for each
150 occurrence was included. The raw data is available for download at <http://goo.gl/2s1geU>.

This raw data was then sorted, cleaned, and manipulated programmatically prior to analysis.
152 Species taxonomic assignments given by the PBDB were updated for accuracy and consistency. For
example, species classified in the order Artiodactyla were reclassified as Cetartiodactyla. These
154 re-assignments follow Smits (2015) and were Janis et al. (2008, 1998) and the Encyclopedia of Life
WEBSITE. Additionally, Taxa who's life habit was classified as either volant (i.e. Chiroptera) or
156 aquatic (e.g. Cetacea) were excluded from this analysis because of both differences in fossilization

potential and applicability to the study of terrestrial species pools.

158 The life habit and dietary categories provided through the PBDB were coarsened to increase per
 159 ecotype sample size; this coarsening follows the same procedure as Smits (2015). Additionally, life
 160 habit category was further modified to break-up the vague “ground-dwelling” category;
 161 re-classifying these species by ankle posture gives more precise information about that species’
 162 environmental context. Ground-dwelling taxa were reassigned following ? by species taxonomic
 163 context. Species ecotype is defined as the interaction between life habit and diet categories. Ecotype
 164 categories with less than 10 species having ever been in that combination were excluded, yielding a
 total of 18 of 24 possible ecotypes.

Table 1: Species trait assignments in this study are a coarser version of the information available in the PBDB. Information was coarsened to improve per category sample size and uniformity and followed this table.

This study		PBDB categories
Diet	Carnivore	Carnivore
	Herbivore	Browser, folivore, granivore, grazer, herbivore.
	Insectivore	Insectivore.
	Omnivore	Frugivore, omnivore.
Locomotor	Arboreal	Arboreal.
	Ground dwelling	Fossorial, ground dwelling, semifossorial, saltatorial.
	Scansorial	Scansorial.

Table 2: Posture assignment based on taxonomy

Order	Family	Stance
	Ailuridae	plantigrade
	Allomyidae	plantigrade
	Amphicyonidae	plantigrade
	Amphilemuridae	plantigrade
	Anthracotheriidae	digitigrade
	Antilocapridae	unguligrade
	Apheliscidae	plantigrade

Continued on next page

Table 2 – continued from previous page

Order	Family	Stance
	Aplodontidae	plantigrade
	Apternodontidae	scansorial
	Arctocyonidae	unguligrade
	Barbourofelidae	digitigrade
	Barylambdidae	plantigrade
	Bovidae	unguligrade
	Camelidae	unguligrade
	Canidae	digitigrade
	Cervidae	unguligrade
	Cimolodontidae	scansorial
	Coryphodontidae	plantigrade
	Cricetidae	plantigrade
	Cylindrodontidae	plantigrade
	Cyriacotheriidae	plantigrade
	Dichobunidae	unguligrade
Dinocerata		unguligrade
	Dipodidae	digitigrade
	Elephantidae	digitigrade
	Entelodontidae	unguligrade
	Eomyidae	plantigrade
	Erethizontidae	plantigrade
	Erinaceidae	plantigrade
	Esthonychidae	plantigrade
	Eutypomyidae	plantigrade
	Felidae	digitigrade

Continued on next page

Table 2 – continued from previous page

Order	Family	Stance
	<i>Florentiamyidae</i>	plantigrade
	<i>Gelocidae</i>	unguligrade
	<i>Geolabididae</i>	plantigrade
	<i>Glyptodontidae</i>	plantigrade
	<i>Gomphotheriidae</i>	unguligrade
	<i>Hapalodectidae</i>	plantigrade
	<i>Heteromyidae</i>	digitigrade
	<i>Hyaenidae</i>	digitigrade
	<i>Hyaenodontidae</i>	digitigrade
	<i>Hypertragulidae</i>	unguligrade
	<i>Ischyromyidae</i>	plantigrade
	<i>Jimomyidae</i>	plantigrade
Lagomorpha		digitigrade
	<i>Leptictidae</i>	plantigrade
	<i>Leptochoeridae</i>	unguligrade
	<i>Leptomerycidae</i>	unguligrade
	<i>Mammutidae</i>	unguligrade
	<i>Megalonychidae</i>	plantigrade
	<i>Megatheriidae</i>	plantigrade
	<i>Mephitidae</i>	plantigrade
	<i>Merycoidodontidae</i>	digitigrade
Mesonychia		unguligrade
	<i>Mesonychidae</i>	digitigrade
	<i>Micropternodontidae</i>	plantigrade
	<i>Mixodectidae</i>	plantigrade

Continued on next page

Table 2 – continued from previous page

Order	Family	Stance
	Moschidae	unguligrade
	Muridae	plantigrade
	Mustelidae	plantigrade
	Mylagaulidae	fossorial
	Mylodontidae	plantigrade
	Nimravidae	digitigrade
	Nothrotheriidae	plantigrade
Notoungulata		unguligrade
	Oromerycidae	unguligrade
	Oxyaenidae	digitigrade
	Palaeomerycidae	unguligrade
	Palaeoryctidae	plantigrade
	Pampatheriidae	plantigrade
	Pantolambdidae	plantigrade
	Peritychidae	digitigrade
Perissodactyla		unguligrade
	Phenacodontidae	unguligrade
Primates		plantigrade
	Procyonidae	plantigrade
	Proscalopidae	plantigrade
	Protoceratidae	unguligrade
	Reithroparamyidae	plantigrade
	Sciuravidae	plantigrade
	Sciuridae	plantigrade
	Simimyidae	plantigrade

Continued on next page

Table 2 – continued from previous page

Order	Family	Stance
	Soricidae	plantigrade
	Suidae	digitigrade
	Talpidae	fossorial
	Tayassuidae	unguligrade
	Tenrecidae	plantigrade
	Titanoideidae	plantigrade
	Ursidae	plantigrade
	Viverravidae	plantigrade
	Zapodidae	plantigrade

166

Species mass information was gathered from multiple different sources where a plurality of the body
168 size estimates are from the PBDB. Body part measurements for many species are also available
through the PBDB. Just as with Smits (2015), these measurements and corresponding regression
170 equations were used to get mass estimates for more species. Additional mass estimates and body
part measurements were sourced from numerous publications and the Neogene Old World Database;
172 see the supplementary material to Smits (2015) for details. Mass was log-transformed and then
mean-centered and rescaled by dividing by two-times its standard deviation; this insures that the
174 magnitude of effects for both continuous and discrete covariates are comparable (Gelman, 2008;
Gelman and Hill, 2007).

176 All fossil occurrences from 64 to 2 million years ago (Mya) were binned into 31 2 million year (My)
bins. This temporal length was chosen because it is approximately the resolution of the North
178 American mammal fossil record.

Table 3: Regression equations used in this study for estimating body size. Equations are presented with reference to taxonomic grouping, part name, and reference.

Group	Equation	log(Measurement)	Source
General	$\log(m) = 1.827x + 1.81$	lower m1 area	Legendre (1986)
General	$\log(m) = 2.9677x - 5.6712$	mandible length	?
General	$\log(m) = 3.68x - 3.83$	skull length	?
Carnivores	$\log(m) = 2.97x + 1.681$	lower m1 length	?
Insectivores	$\log(m) = 1.628x + 1.726$	lower m1 area	?
Insectivores	$\log(m) = 1.714x + 0.886$	upper M1 area	?
Lagomorph	$\log(m) = 2.671x - 2.671$	lower toothrow area	Tomiya (2013)
Lagomorph	$\log(m) = 4.468x - 3.002$	lower m1 length	Tomiya (2013)
Marsupials	$\log(m) = 3.284x + 1.83$	upper M1 length	?
Marsupials	$\log(m) = 1.733x + 1.571$	upper M1 area	?
Rodentia	$\log(m) = 1.767x + 2.172$	lower m1 area	Legendre (1986)
Ungulates	$\log(m) = 1.516x + 3.757$	lower m1 area	?
Ungulates	$\log(m) = 3.076x + 2.366$	lower m2 length	?
Ungulates	$\log(m) = 1.518x + 2.792$	lower m2 area	?
Ungulates	$\log(m) = 3.113x - 1.374$	lower toothrow length	?

Environmental and temporal covariates

- 180 The group-level covariates in this study are descriptors of species' environmental context,
 specifically global temperature estimates and Graham's floral intervals CITATION. Global
 182 temperature across most of the Cenozoic was calculated from Mg/Ca isotope record from deep sea
 carbonates (Cramer et al., 2011). Mg/Ca based temperature estimates are preferable to the
 184 frequently used $\delta^{18}\text{O}$ temperature proxy (Alroy et al., 2000; Figueirido et al., 2012; Zachos et al.,
 2008, 2001) because Mg/Ca estimates do not conflate temperature with ice sheet volume and
 186 depth/stratification changes; this makes it preferable as an estimate of global temperature for
 macroevolutionary and macroecological studies (Ezard et al., 2016).
- 188 Two aspects of the Mg/Ca-based temperature curve were included in this analysis: mean and range.
 Both were calculated as the mean of all respective estimates for each 2 My temporal bins. Both
 190 mean and range were then rescaled as above: subtract mean, divide by twice the standard deviation.
- The other major set of environmental factors included in this study are Graham's Cenozoic plant
 192 phases CITATION. Graham's plant phases are holistic descriptors of the taxonomic composition of

		State at $t + 1$		
		0_{never}	1	$0_{extinct}$
State at t	0_{never}	$1 - \theta$	θ	0
	1	0	θ	$1 - \theta$
	$0_{extinct}$	0	0	1

(a) Pure-presence

		State at $t + 1$		
		0_{never}	1	$0_{extinct}$
State at t	0_{never}	$1 - \phi$	ϕ	0
	1	0	π	$1 - \pi$
	$0_{extinct}$	0	0	1

(b) Birth-death

Table 4: Transition matrices for the pure-presence (4a) and birth-death (4b) models. Both of these models share the core machinery of discrete-time birth-death processes but make distinct assumptions about the equality of originating and surviving (Eq. 2, and 3). Note also that while there are only two state “codes” (0, 1), there are in fact three states: never having originated 0_{never} , present 1, extinct $0_{extinct}$ (Allen, 2011).

12 ecosystem types, which plants are present at a given time, and the relative modernity of those
 194 plant groups with younger phases representing increasingly modern taxa CITATION. Graham
 CITATION defines four intervals from the Cretaceous to the Pliocene, though only three of these
 196 intervals are included in this analysis. Graham’s plant phases CITATION was included as a series
 of “dummy variables” encoding the three phases included in this analysis. This means that the first
 198 phase is synonymous with the intercept and phases

Modelling species occurrence

200 Two different models were used in this study: a pure-presence model and a birth-death model. Both
 models at their core are hidden Markov model where the latent aspect of the process has an
 202 absorbing state (Allen, 2011). The difference between these two models is if the probability of a
 species origination and survival are considered equal or different (Table 4). Something that is
 204 important to realize is that while there are only two state “codes” in a presence-absence matrix (i.e.
 0/1), there are in fact three states in a birth-death model: never having originated, extant, and
 206 extinct. The last of these is the absorbing state, as once a species has gone extinct it cannot
 re-originate (Allen, 2011); this is made obvious in the transition matrices as the probability of an
 208 extinct species changing states is 0 (Table 4). See below for parameter explanations (Tables 6, and
 7).

210 **Data augmentation**

All presence/absence observations are incomplete. The hidden Markov model at the core of this
212 analysis allows for observed absences to be used meaningfully to estimate the number of unobserved
species. Of specific concern in this analysis is the unknown “true” size of the dataset; how many
214 species could have actually been observed? While many species have been observed, the natural
incompleteness of all observations, especially in the case of paleontological data, there are obviously
216 many species which were never sampled (Royle and Dorazio, 2008; Royle et al., 2007).

Let N by the total number of observed species, M be the upper limit of possible species that could
218 have existed given a model of species presence, and N^* is the all-zero histories where $N^* = M - N$.
This approach assumes that $\hat{N} \sim \text{Binomial}(M, \psi)$ where \hat{N} is the estimated “true” number of
220 species and ψ is the probability that any augmented species should actually be “present.” Because
 M is user defined, this approach effectively gives ψ a uniform prior over N to M (Royle and
222 Dorazio, 2008). For this study, $M = N + \lfloor N/4 \rfloor$.

Data imputation is the process of estimating missing data for partially observed covariates (Gelman
224 and Hill, 2007; Rubin, 1996), this is simple in a Bayesian context because data are also parameters
(Gelman et al., 2013). Augmented species also have no known mass so a mass estimate must be
226 imputed for each possible species (Royle and Dorazio, 2012). This procedure assumes that mass
values for augmented species are from the same distribution as observed species. The distribution of
228 observed mass values is estimated as part of the model, and new mass values are then generated
from this distribution. This approach is an example of imputing data missing completely at random
230 (Gelman and Hill, 2007; Royle and Dorazio, 2012). Because log mass values are rescaled as a part of
this study, the body mass distribution is already known ($\mathcal{N}(0, 0.5)$); augmented species body mass
232 just simply drawn from this distribution.

In addition to body mass information, the augmented species need an ecotype classification. Because
234 these species are completely unknown, they were all classified as “augmented,” an additional
grouping indicating their unknown biology. This classification has no biological interpretation.

Table 5: Observation parameters

Parameter	dimensions	explanation
y	$N \times T$	observed species presence/absence
z	$N \times T$	“true” species presence/absence
p	T	probability of observing a species that is present at time t
m	N	species log mass, rescaled
α_0	1	average log-odds of p
α_1	1	change in average log-odds of p per change mass
r	T	difference from α_0 associated with time t
σ	1	standard deviation of r

236 Observation process

- The type of hidden Markov model used in this study has three characteristic probabilities:
- 238 probability p of observing a species given that it is present, probability ϕ of a species surviving from one time to another, and probability π of a species first appearing (Royle and Dorazio, 2008). In
240 this formulation, the probability of a species going extinct is $1 - \pi$. For the pure-presence model
 $\phi = \pi$, while for the birth-death model $\phi \neq \pi$.
- 242 The probability of observing a species that is present p is modeled as a logistic regression was a time-varying intercept and species mass as a covariate. The effect of species mass on p was assumed
244 linear and constant over time and given a prior reflecting a possible positive relationship; these assumptions are reflected in the structure of the model Equation 1. The parameters associated with
246 this part of the model are described in Table 5.

$$\begin{aligned}
y_{i,t} &\sim \text{Bernoulli}(p_{i,t} z_{i,t}) \\
p_{i,t} &= \text{logit}^{-1}(\alpha_0 + \alpha_1 m_i + r_t) \\
r_t &\sim \mathcal{N}(0, \sigma)
\end{aligned} \tag{1}$$

Pure-presence process

- 248 For the pure-presence model there is only a single probability dealing with the presence of a species θ (Table 4a). This probability was modeled as multi-level logistic regression with both species-level

Table 6: Parameters for the model of presence in the pure-presence model

Parameter	dimensions	explanation
z	$N \times T$	“true” species presence/absence
θ	$N \times T - 1$	probability of $z = 1$
a	$T - 1 \times D$	ecotype-varying intercept; mean value of log-odds of θ
m	N	species log mass, rescaled
b_1	1	effect of species mass on log-odds of θ
b_2	1	effect of species mass, squared, on log-odds of θ
U	$T \times D$	matrix of group-level covariates
γ	$U \times D$	matrix of group-level regression coefficients
Σ	$D \times D$	covariance matrix of a
Ω	$D \times D$	correlation matrix of a
τ	D	vector of standard deviations for each ecotype a_d

250 and group-level covariates (Gelman et al., 2013; Gelman and Hill, 2007). The parameters associated
with pure-presence model are presented in Table 6 and the full sampling statement in Equation 2.

252 The species-level of the model (Eq. 2) is a logistic regression with varying-intercept that varies by
ecotype. Additionally, species mass was included as a covariate associated with two regression
254 coefficients allowing a quadratic relationship with log-odds of occurrence. This assumption is based
on the known distribution of mammal body masses where species with intermediate mass values are
256 more common than either small or large bodied species. These assumptions are also reflected in the
choice of priors for these regression coefficients.

258 The values of each ecotype’s intercept are themselves modeled as regressions using the group-level
covariates associated with environmental context. Each of these regressions has an associated
260 variance of possible values of each ecotype’s intercept (Gelman and Hill, 2007). In addition, the
covariances between ecotype intercepts, given this group-level regression, are modeled (Gelman and
262 Hill, 2007).

All parameters not modeled elsewhere were given weakly informative priors (Gelman et al., 2013)
264 CITATION STAN MANUAL STATISTICAL RETHINKING. Weakly informative means that
priors do not necessarily encode actual prior information but instead help regularize or weakly
266 constrain posterior estimates. These priors have a concentrated probability density around and near
zero; this has the effect of tempering our estimates and help prevent overfitting the model to the

268 data (Gelman et al., 2013) CITATION STAN MANUAL STATISTICAL RETHINKING.

$$\begin{aligned} y_{i,t} &\sim \text{Bernoulli}(p_{i,t} z_{i,t}) & \alpha_0 &\sim \mathcal{N}(0, 1) \\ p_{i,t} &= \text{logit}^{-1}(\alpha_0 + \alpha_1 m_i + r_t) & \alpha_1 &\sim \mathcal{N}(1, 1) \\ r_t &\sim \mathcal{N}(0, \sigma) & \sigma &\sim \mathcal{N}^+(1) \\ z_{i,1} &\sim \text{Bernoulli}(\rho) & b_1 &\sim \mathcal{N}(0, 1) \\ z_{i,t} &\sim \text{Bernoulli}(\theta_{i,t}) & b_2 &\sim \mathcal{N}(-1, 1) \\ \theta_{i,t} &= \text{logit}^{-1}(a_{t,j[i]} + b_1 m_i + b_2 m_i^2) & \gamma &\sim \mathcal{N}(0, 1) \\ a &\sim \text{MVN}(u\gamma, \Sigma) & \tau &\sim \mathcal{N}^+(1) \\ \Sigma &= \text{diag}(\tau)\Omega\text{diag}(\tau) & \Omega &\sim \text{LKJ}(2) \end{aligned} \tag{2}$$

Birth-death process

- 270 In the birth-death model, $\phi \neq \pi$ and so each of these probabilities are modeled separately but in a
similar manner to how θ is modeled in the pure-presence model (Eq. 2, Table 4b). The parameters
272 associated with the birth-death presence model are presented in Table 7 and the full sampling
statement, including observation (Eq. 1), is described in Equation 3.
- 274 Similar to the pure-presence model, both ϕ and π are modeled as logistic regressions with
varying-intercept and one covariate associated with two parameters. The possible relationships
276 between mass and both ϕ and π are reflected in the parameterization of the model and choice of
priors (Eq. 3).
- 278 The intercepts of ϕ and π both vary by species ecotype and those values are themselves the product
of group-level regression using environmental factors as covariates (Eq. 3); this is identical to the

Table 7: Parameters for the model of presence in the pure-presence model

Parameter	dimensions	explanation
z	$N \times T$	“true” species presence/absence
ϕ	$N \times T$	probability of $z_{-,t} = 1 z_{-,t-1} = 0$
π	$N \times T - 1$	probability of $z_{-,t} = 1 z_{-,t-1} = 1$
a^ϕ	$T - 1 \times D$	ecotype-varying intercept; mean value of log-odds of θ
a^π	$T - 1 \times D$	ecotype-varying intercept; mean value of log-odds of θ
m	N	species log mass, rescaled
b_1^ϕ	1	effect of species mass on log-odds of ϕ
b_1^π	1	effect of species mass on log-odds of π
b_2^ϕ	1	effect of species mass, squared, on log-odds of ϕ
b_2^π	1	effect of species mass, squared, on log-odds of π
U	$T \times D$	matrix of group-level covariates
γ^ϕ	$U \times D$	matrix of group-level regression coefficients
γ^π	$U \times D$	matrix of group-level regression coefficients
Σ^ϕ	$D \times D$	covariance matrix of a^ϕ
Σ^π	$D \times D$	covariance matrix of a^π
Ω^ϕ	$D \times D$	correlation matrix of a^ϕ
Ω^π	$D \times D$	correlation matrix of a^π
τ^ϕ	D	vector of standard deviations for each ecotype a_d^ϕ
τ^π	D	vector of standard deviations for each ecotype a_d^π

280 pure presence model (Eq. 2).

$$\begin{aligned}
 y_{i,t} &\sim \text{Bernoulli}(p_{i,t} z_{i,t}) & \Sigma^\phi &= \text{diag}(\tau^\phi) \Omega^\phi \text{diag}(\tau^\phi) \\
 p_{i,t} &= \text{logit}^{-1}(\alpha_0 + \alpha_1 m_i + r_t) & \Sigma^\pi &= \text{diag}(\tau^\pi) \Omega^\pi \text{diag}(\tau^\pi) \\
 r_t &\sim \mathcal{N}(0, \sigma) & \rho &\sim U(0, 1) \\
 \alpha_0 &\sim \mathcal{N}(0, 1) & b_1^\phi &\sim \mathcal{N}(0, 1) \\
 \alpha_1 &\sim \mathcal{N}(1, 1) & b_1^\pi &\sim \mathcal{N}(0, 1) \\
 \sigma &\sim \mathcal{N}^+(1) & b_2^\phi &\sim \mathcal{N}(-1, 1) \\
 z_{i,1} &\sim \text{Bernoulli}(\phi_{i,1}) & b_2^\pi &\sim \mathcal{N}(-1, 1) \\
 z_{i,t} &\sim \text{Bernoulli} \left(z_{i,t-1} \pi_{i,t} + \sum_{x=1}^t (1 - z_{i,x}) \phi_{i,t} \right) & \gamma^\phi &\sim \mathcal{N}(0, 1) \\
 \phi_{i,t} &= \text{logit}^{-1}(a_{t,j[i]}^\phi + b_1^\phi m_i + b_2^\phi m_i^2) & \tau^\phi &\sim \mathcal{N}^+(1) \\
 \pi_{i,t} &= \text{logit}^{-1}(a_{t,j[i]}^\pi + b_1^\pi m_i + b_2^\pi m_i^2) & \tau^\pi &\sim \mathcal{N}^+(1) \\
 a^\phi &\sim \text{MVN}(U\gamma^\phi, \Sigma^\phi) & \Omega^\phi &\sim \text{LKJ}(2) \\
 a^\pi &\sim \text{MVN}(U\gamma^\pi, \Sigma^\pi) & \Omega^\pi &\sim \text{LKJ}(2)
 \end{aligned} \tag{3}$$

Posterior inference and model adequacy

282 Programs that implement joint posterior inference for the above models (Eqs. 2, 3) were
283 implemented in the probabilistic programming language Stan CITATION. The models used here
284 both feature latent discrete parameters in the large matrix z (Tables 5, 6, 7; Eqs. 1, 2, 3). All
285 methods for posterior inference implemented in Stan are derivative based which causes
286 complications for actually implementing the above models because integers do not have derivatives.
287 Instead of implementing a latent discrete parameterization, the posterior probabilities of all possible
288 states of the latent parameters z were estimated (i.e. marginalized).

Species durations at minimum range-through from the FAD to the LAD, but the incompleteness of
290 all observations means that the actual time of origination or extinction is unknown. The
marginalization approach used here means that the probabilities all possible histories for a species
292 are calculated, from the end members of the species having existed for the entire study interval and
the species having only existed between the directly observed FAD and LAD to all possible
294 intermediaries CITATION STAN MANUAL.

The combined size of the dataset and large number of parameters in both models (Eqs. 2, 3),
296 specifically the total number of latent parameters that are the matrix z , means that stochastic
approximate posterior inference is computationally very slow even using HMC. Instead, an
298 approximate Bayesian approach was used: variational inference. A recently developed automatic
variational inference algorithm called “automatic differentiation variational inference” (ADVI) is
300 implemented in Stan and was used here CITATION. ADVI assumes that the posterior is Gaussian
but still yields a true Bayesian posterior; this assumption is similar to quadratic approximation of
302 the likelihood function used in maximum likelihood inference CITATION. The principal limitation
of assuming the joint posterior is Gaussian is that the true topology of the log-posterior isn’t
304 estimated; this is a particular burden for scale parameters which are bound to be positive (e.g.
standard deviation).

306 After fitting both models (Eqs. 2, 3) using ADVI, model adequacy and quality of fit was assessed
using a series of posterior predictive checks CITATION CITATION. Because all Bayesian models

308 are inherently generative, simulations of new data sets is “free” CITATION. By simulating many
 310 theoretical data sets using the observed covariate information the congruence between predictions
 311 made by the model and the observed empirical data can be assessed. By combining multiple
 312 posterior predictive tests of congruence between empirical and simulated values of interest, the
 holistic adequacy of the model can be analyzed CITATION.

An example posterior predictive check used in this study was comparing the observed average
 314 number of observations per species to a distribution of simulated averages; if the empirically
 observed value sits in the middle of the distribution than the model is adequate in reproducing the
 316 observed number of occurrences per species.

Posterior simulations for time series are start with the values at $t = 1$ and then just simulating
 318 forward.

Given parameter estimates, diversity and diversification rates are estimated through posterior
 320 predictive simulations. Given the observed presence-absence matrix y , estimates of the true
 presence-absence matrix z can be simulated and the distribution of possible occurrence histories
 322 can be analyzed. This is conceptually similar to marginalization where the probability of each
 possible occurrence history is estimated (Fig. 2).

324 The posterior distribution of z gives the estimate of standing diversity N_t^{stand} for all time points as

$$N_t^{stand} = \sum_{i=1}^M z_{i,t}. \quad (4)$$

Given estimates of N^{stand} for all time points, the estimated number of originations O_t are be
 326 estimated as

$$O_t = \sum_{i=1}^M z_{i,t} = 1 | z_{i,t-1} = 0 \quad (5)$$

and number of extinctions E_t estimated as

$$E_t = \sum_{i=1}^M z_{i,t} = 0 | z_{i,t-1} = 1. \quad (6)$$

³²⁸ Per-capita growth D^{rate} , origination O^{rate} and extinction E^{rate} rates are then calculated as

$$\begin{aligned} O_t^{rate} &= \frac{O_t}{N_{t-1}^{stand}} \\ E_t^{rate} &= \frac{E_t}{N_{t-1}^{stand}} \\ D_t^{rate} &= O_t^{rate} - E_t^{rate}. \end{aligned} \tag{7}$$

Results

³³⁰ Posterior results take one of two forms: direct inspection of parameter estimates, and downstream estimates of diversity and diversification rates. For the former, both the pure-presence and
³³² birth-death models (Eq. 2, and 3 are inspected. For the latter, only posterior estimates from the birth-death model are considered; the reason for this is explained below in the comparison of the
³³⁴ models' posterior predictive check results.

Comparing parameter estimates from the pure-presence and birth-death models

Comparison of the posterior predictive performance of the pure-presence and birth-death models
³³⁸ reveals a striking difference in quality of the models' fits to the data (Fig. 3a and 3b). The birth-death model is clearly able to reproduce the observed average number of occurrence, in
³⁴⁰ contrast to the pure-birth model which greatly underestimates the ovserved average number of occurrences. The interpretation of these results is that the results of the birth-death model are
³⁴² more representative of the data than the pure-presence model, though further inspection of the posterior parameter estimates can provide further insight into why these models give different
³⁴⁴ posterior predictive results (Gelman et al., 2013). However, it is expected that downstream analyses from the birth-death model will be more reliable than that from the pure-presence model.
³⁴⁶ Occurrence probabilities estimated from the pure-presence model (Fig. 4) are broadly similar to the estimates of origination probability from the birth-death model (Fig. 5) as opposed to the estimates

348 of survival probability (Fig. 6). This result supports the idea that changes to the North American
regional species pool is more likely due to changes to origination than extinction.

350 For most ecotypes, both estimated occurrence probabilities from the pure-presence model (Fig. 4)
and origination probabilities estimated from the birth-death model (Fig. 5) increase with time.

352 Notably, ecotypes with arboreal components do not appear to follow a similar pattern; instead,
occurrence and origination probabilities appear relatively flat for most of the Cenozoic.

354 The dramatic differences between origination and survival probabilities indicate how different these
processes are, and may be responsible for the better posterior predictive performance of the

356 birth-death model over the pure-presence model (Fig. 3a, and 3b). While the estimates of both time
series have high variance, what is striking is how mean origination probability changes over time

358 while most ecotype survival probabilities have relatively stable means for the entire Cenozoic (Fig.
5, and 6).

360 For most ecotypes, the estimates of origination probabilities are with less uncertainty than similar
estimates of survival probabilities (Fig. 5, and 6). High uncertainty in the estimates of the

362 underlying log-odds of occurrence, origination, or survival tends to be indicative of extreme rarity
or complete absence of the specific ecotype; the latter is called complete separation, the effect of

364 which has been mitigated by the hierarchical modeling strategy used here (Gelman et al., 2013;
Gelman and Hill, 2007) CITATION Statistical Rethinking.

366 The pure-presence and birth-death models differ in estimated effect of mass on the probability of
sampling a species that is present (Fig. 7). For the pure-presence model, mass is estimated to have

368 not have a great effect on the probability of sampling a species that is present (Fig. 7a).

Contrastingly, for the birth-death model mass is found to have a negative relationship with

370 observation such that larger species are less likely to be observed if present than smaller species
(Fig. 7b).

372 The result from the birth-death model is unexpected given that it is generally assumed that larger
mammals are more likely to have been collected than smaller mammals CITATION. However,

374 collection is not preservation; similarities in preservation rate indicate similarities in how gap-filled

species records are. What this result means is that the record of large bodied species is expected on
376 average to be more gap-filled and less consistent from time point to time point than smaller bodied
species. Additionally, this is presence/absence data, so higher preservation and collection in terms
378 of individual specimens at a location or a single temporal horizon does not necessarily translate to
high preservation over time.

380 The average probabilities of sampling for both the pure-presence model and birth-death model are
both at the point where (rescaled log) mass equals 0; visual comparison indicates that, on average,
382 sampling probability has greater posterior estimate in the pure-presence model than the birth-death
model (Fig. 7).

384 The effect of species mass on probability of occurrence as estimated from the pure-presence (Fig. 8)
are most similar to the estimated effect of species mass on probability of origination for the
386 birth-death model (Fig. 9). The striking pattern observable in both sets of estimates is the higher
probability of occurrence for species with body sizes closer to the mean than either extremes. This
388 result is consistent with the canonically normal distribution of mammal body sizes CITATION; it is
then expected that the most likely to occur species would be those from the middle of the
390 distribution, and that species originating will on average be of average mass, especially considering
species shared common ancestry CITATION. Note that all variation between ecotypes (Fig. 9) is
392 due to differences in ecotype-specific survival probability and the associated effects of plant phase;
the effect of mass was considered constant for all ecotypes.

394 In contrast, the effect of species mass on probability of survival as estimated from the birth-death
model (Fig. 10) indicates little effect of mass on extinction; this is consistent with previous findings
396 from the North American mammal fossil record (Smits, 2015; Tomiya, 2013). Note that all variation
between ecotypes (Fig. 10) is due to differences in ecotype-specific survival probability and the
398 associated effects of plant phase; the effect of mass was considered constant for all ecotypes.

Similarities in parameters estimates between ecotypes may be due to similar response to
400 environmental factors. Some of the obvious patterns from inspection of the individual-level
estimates of occurrence (Fig. 4), origination (Fig. 5), and survival probabilities (Fig. 6) that are of

⁴⁰² note are the similarities between arboreal taxa and the differences between arboreal and all other
taxa.

⁴⁰⁴ Analysis of diversity

All of the following analyses of diversification and macroevolutionary rates has been done using
⁴⁰⁶ only the birth-death model; this is because of the models better posterior predictive check
performance (Fig. 3a, and 3b).

⁴⁰⁸ The general pattern of total estimated North American mammal diversity for the Cenozoic is
“stable” meaning that mean standing diversity does not fluctuate wildly over the Cenozoic (Fig.
⁴¹⁰ 14a). In broad strokes, the first 15 or so million years of the Cenozoic are characterized by a gradual
decline in standing diversity until approximately 45-50 million years ago (early-middle Eocene).
⁴¹² Following this decline, standing diversity is broadly constant from 45 to 18 Mya (early Miocene).
After this, there is a rapid spike in diversity followed by a slight decline in diversity up to the
⁴¹⁴ Modern. This characterization of the estimated diversity history is knowingly broad strokes and
diversity time series is not without variation and vagaries.
⁴¹⁶ When viewed through the lens of diversification rate, some of the structure behind the estimated
diversity history begins to take shape (Fig. 14b). For most of the Cenozoic, the diversification rate
⁴¹⁸ hovers around zero, punctuated by both positive and negative spikes. The largest spike in
diversification rate is at 16 Mya, which is early Oligocene (Fig. 14b). Other notable increases in
⁴²⁰ diversification rate occur at 54, 44, 36, 26, and 20 Mya; other possible increases in diversification
rate are less certain (e.g. 8 Mya). Notable decreases in diversification rate occur at 52, 48, 42, 32,
⁴²² 14, 10, and 6 Mya.

The comparison between per capita origination and extinction rate estimates reveals how
⁴²⁴ diversification rate is formed (Fig. 14c, 14d). Diversification rate seems most driven by changes in
origination rate as opposed to extinction rate. Extinction rate, on the other hand, demonstrates an
⁴²⁶ almost saw-toothed pattern around a constant mean.

Now ask what origin or extinct are doing at the important time points indicated above.

⁴²⁸ Increases in diversification rate at 54, 44, 36, 26, 20, 16

Decreases in diversification rate at 52, 48, 42, 32, 14, 10, 6

⁴³⁰ Diversity partitioned by ecotype reveals a lot of the complexity behind the pattern of mammal diversity for the Cenozoic (Fig. 15).

⁴³² Arboreal ecotypes obtain peak diversity early in the Cenozoic and then decline for the rest of the time series, becoming increasingly rare or absent as diversity approaches the Modern (Fig. 15).

⁴³⁴ Arboreal herbivores and omnivores obtain peak diversity at the beginning of the Cenozoic then go into decline while still possibly remaining a part of the species pool, while arboreal carnivores and

⁴³⁶ insectivores obtain peak diversity 52-50 Mya and then quickly decline and become extremely rare or absent from the species pool.

⁴³⁸ Discussion

Acknowledgements

⁴⁴⁰ I would like to thank K. Angielczyk, M. Foote, P. D. Polly, and R. Ree for helpful discussion and advice. This entire study would not have been possible without the Herculean effort of the

⁴⁴² many contributors to the Paleobiology Database. In particular, I would like to thank J. Alroy and M. Uhen for curating most of the mammal occurrences recorded in the PBDB. This is Paleobiology

⁴⁴⁴ Database publication XXX.

References

⁴⁴⁶ Allen, L. J. S. 2011. An introduction to stochastic processes with applications to biology. 2nd ed. Chapman and Hall/CRC, Boca Raton, FL.

- 448 Alroy, J. 1996. Constant extinction, constrained diversification, and uncoordinated stasis in North
American mammals. *Palaeogeography, Palaeoclimatology, Palaeoecology* 127:285–311.
- 450 ———. 2009. Speciation and extinction in the fossil record of North American mammals. Pages
302–323 *in* R. K. Butlin, J. R. Bridle, and D. Schluter, eds. *Speciation and patterns of diversity*.
452 Cambridge University Press, Cambridge.
- Alroy, J., P. L. Koch, and J. C. Zachos. 2000. Global climate change and North American
454 mammalian evolution. *Paleobiology* 26:259–288.
- Badgley, C., and J. A. Finarelli. 2013. Diversity dynamics of mammals in relation to tectonic and
456 climatic history: comparison of three Neogene records from North America. *Paleobiology*
39:373–399.
- 458 Bambach, R. K. 1977. Species richness in marine benthic habitats through the Phanerozoic.
Paleobiology 3:152–167.
- 460 Bambach, R. K., A. M. Bush, and D. H. Erwin. 2007. Autecology and the filling of ecospace: Key
metazoan radiations. *Palaeontology* 50:1–22.
- 462 Blois, J. L., and E. A. Hadly. 2009. Mammalian Response to Cenozoic Climatic Change. *Annual
Review of Earth and Planetary Sciences* 37:181–208.
- 464 Brown, A. M., D. I. Warton, N. R. Andrew, M. Binns, G. Cassis, and H. Gibb. 2014. The
fourth-corner solution - using predictive models to understand how species traits interact with
466 the environment. *Methods in Ecology and Evolution* 5:344–352.
- Bush, A. M., and R. K. Bambach. 2011. Paleoenvironmental Megatrends in Marine Metazoa, vol. 39.
- 468 Bush, A. M., R. K. Bambach, and G. M. Daley. 2007. Changes in theoretical ecospace utilization in
marine fossil assemblages between the mid-Paleozoic and late Cenozoic. *Paleobiology* 33:76–97.
- 470 Clyde, W. C., and P. D. Gingerich. 1998. Mammalian community response to the latest Paleocene
thermal maximum: an isotaphonomic study in the northern Bighorn Basin, Wyoming. *Geology*
472 26:1011–1014.

- Cramer, B. S., K. Miller, P. Barrett, and J. Wright. 2011. Late Cretaceous-Neogene trends in deep
474 ocean temperature and continental ice volume: Reconciling records of benthic foraminiferal
geochemistry ($\delta^{18}\text{O}$ and Mg/Ca) with sea level history. *Journal of Geophysical Research: Oceans*
476 116:1–23.
- Eronen, J. T., C. M. Janis, C. P. Chamberlain, and A. Mulch. 2015. Mountain uplift explains
478 differences in Palaeogene patterns of mammalian evolution and extinction between North
America and Europe. *Proceedings of the Royal Society B: Biological Sciences* 282:20150136.
- Ezard, T. H. G., A. Purvis, and H. Morlon. 2016. Environmental changes define ecological limits to
480 species richness and reveal the mode of macroevolutionary competition. *Ecology Letters*
482 19:899–906.
- Figueirido, B., C. M. Janis, J. A. Pérez-Claros, M. De Renzi, and P. Palmqvist. 2012. Cenozoic
484 climate change influences mammalian evolutionary dynamics. *Proceedings of the National
Academy of Sciences* 109:722–727.
- Foote, M. 2001. Inferring temporal patterns of preservation, origination, and extinction from
486 taxonomic survivorship analysis. *Paleobiology* 27:602–630.
- Foote, M., and J. J. Sepkoski. 1999. Absolute measures of the completeness of the fossil record.
Nature 398:415–7.
- Gelman, A. 2008. Scaling regression inputs by dividing by two standard deviations. *Statistics in
490 Medicine* pages 2865–2873.
- Gelman, A., J. B. Carlin, H. S. Stern, D. B. Dunson, A. Vehtari, and D. B. Rubin. 2013. Bayesian
492 data analysis. 3rd ed. Chapman and Hall, Boca Raton, FL.
- Gelman, A., and J. Hill. 2007. Data Analysis using Regression and Multilevel/Hierarchical Models.
494 Cambridge University Press, New York, NY.
- Jamil, T., W. A. Ozinga, M. Kleyer, and C. J. F. Ter Braak. 2013. Selecting traits that explain
496

- species-environment relationships: A generalized linear mixed model approach. *Journal of*
498 *Vegetation Science* 24:988–1000.
- Janis, C., J. Damuth, and J. M. Theodor. 2004. The species richness of Miocene browsers, and
500 implications for habitat type and primary productivity in the North American grassland biome.
Palaeogeography, Palaeoclimatology, Palaeoecology 207:371–398.
- 502 Janis, C. M. 1993. Tertiary mammal evolution in the context of changing climates, vegetation, and
tectonic events. *Annual Review of Ecology and Systematics* 24:467–500.
- 504 ———. 2008. An evolutionary history of browsing and grazing ungulates. Pages 21–45 *in* I. J.
Gordon and H. H. T. Prins, eds. *The Ecology of Browsing and Grazing*. Springer-Verlag.
- 506 Janis, C. M., J. Damuth, and J. M. Theodor. 2000. Miocene ungulates and terrestrial primary
productivity: where have all the browsers gone? *Proceedings of the National Academy of Sciences*
508 97:7899–904.
- Janis, C. M., G. F. Gunnell, and M. D. Uhen. 2008. Evolution of Tertiary mammals of North
510 America. Vol. 2. Small mammals, xenarthrans, and marine mammals. Cambridge University
Press, Cambridge.
- 512 Janis, C. M., K. M. Scott, and L. L. Jacobs. 1998. Evolution of Tertiary mammals of North
America. Vol. 1. Terrestrial carnivores, ungulates, and ungulate-like mammals. Cambridge
514 University Press, Cambridge.
- Janis, C. M., and P. B. Wilhelm. 1993. Were there mammalian pursuit predators in the tertiary?
516 Dances with wolf avatars. *Journal of Mammalian Evolution* 1:103–125.
- Jernvall, J., and M. Fortelius. 2004. Maintenance of trophic structure in fossil mammal
518 communities: site occupancy and taxon resilience. *The American Naturalist* 164:614–624.
- Legendre, S. 1986. Analysis of mammalian communities from the Late Eocene and Oligocene of
520 Southern France. *Paleovertebrata* 16:191–212.
- Liow, L. H., M. Fortelius, E. Bingham, K. Lintulaakso, H. Mannila, L. Flynn, and N. C. Stenseth.

- 522 2008. Higher origination and extinction rates in larger mammals. *Proceedings of the National
Academy of Sciences* 105:6097–6102.
- 524 Liow, L. H., M. Fortelius, K. Lintulaakso, H. Mannila, and N. C. Stenseth. 2009. Lower Extinction
Risk in SleeporHide Mammals. *The American Naturalist* 173:264–272.
- 526 Lloyd, G. T., J. R. Young, and A. B. Smith. 2011. Taxonomic Structure of the Fossil Record is
Shaped by Sampling Bias. *Systematic Biology* 61:80–89.
- 528 Pires, M. M., D. Silvestro, and T. B. Quental. 2015. Continental faunal exchange and the
asymmetrical radiation of carnivores. *Proceedings of the Royal Society B: Biological Sciences*
530 282:20151952.
- 532 Pollock, L. J., W. K. Morris, and P. A. Vesk. 2012. The role of functional traits in species
distributions revealed through a hierarchical model. *Ecography* 35:716–725.
- 534 Quental, T. B., and C. R. Marshall. 2013. How the Red Queen Drives Terrestrial Mammals to
Extinction. *Science* 341:290–292.
- 536 Royle, J. A., and R. M. Dorazio. 2008. Hierarchical modeling and inference in ecology: the analysis
of data from populations, metapopulations and communities. Elsevier, London.
- 538 ———. 2012. Parameter-expanded data augmentation for Bayesian analysis of capture-recapture
models. *Journal of Ornithology* 152:521–537.
- 540 Royle, J. A., R. M. Dorazio, and W. a. Link. 2007. Analysis of Multinomial Models With Unknown
Index Using Data Augmentation. *Journal of Computational and Graphical Statistics* 16:67–85.
- 542 Royle, J. A., J. D. Nichols, M. Kéry, E. Ranta, and M. Kery. 2014. detection is of species when
Modelling occurrence and abundance imperfect 110:353–359.
- Rubin, D. B. 1996. Multiple imputation after 18+ years. *Journal of the American Statistical
Assocaition* 91:473–489.
- Silvestro, D., A. Antonelli, N. Salamin, and T. B. Quental. 2015. The role of clade competition in

- 546 the diversification of North American canids. *Proceedings of the National Academy of Sciences of*
the United States of America 112:8684–9.
- 548 Slater, G. J. 2015. Iterative adaptive radiations of fossil canids show no evidence for
diversity-dependent trait evolution. *Proceedings of the National Academy of Sciences*
550 112:4897–4902.
- 552 Smits, P. D. 2015. Expected time-invariant effects of biological traits on mammal species duration.
Proceedings of the National Academy of Sciences 112:13015–13020.
- 554 Strömberg, C. A. E. 2005. Decoupled taxonomic radiation and ecological expansion of open-habitat
grasses in the Cenozoic of North America. *Proceedings of the National Academy of Sciences of*
the United States of America 102:11980–4.
- 556 Tomiya, S. 2013. Body Size and Extinction Risk in Terrestrial Mammals Above the Species Level.
The American Naturalist 182:196–214.
- 558 Valentine, J. W. 1969. Patterns of taxonomic and ecological structure of the shelf benthos during
Phanerozoic time. *Paleontology* 12:684–709.
- 560 Wang, S. C., P. J. Everson, H. J. Zhou, D. Park, and D. J. Chudzicki. 2016. Adaptive credible
intervals on stratigraphic ranges when recovery potential is unknown. *Paleobiology* 42:240–256.
- 562 Wang, S. C., and C. R. Marshall. 2016. Estimating times of extinction in the fossil record. *Biology*
Letters 12:20150989.
- 564 Warton, D. I., B. Shipley, and T. Hastie. 2015. CATS regression - a model-based approach to
studying trait-based community assembly. *Methods in Ecology and Evolution* 6:389–398.
- 566 Zachos, J. C., G. R. Dickens, and R. E. Zeebe. 2008. An early Cenozoic perspective on greenhouse
warming and carbon-cycle dynamics. *Nature* 451:279–283.
- 568 Zachos, J. C., M. Pagani, L. Sloan, E. Thomas, and K. Billups. 2001. Trends, rhythms, and
aberrations in global climate 65 Ma to present. *Science* 292:686–693.

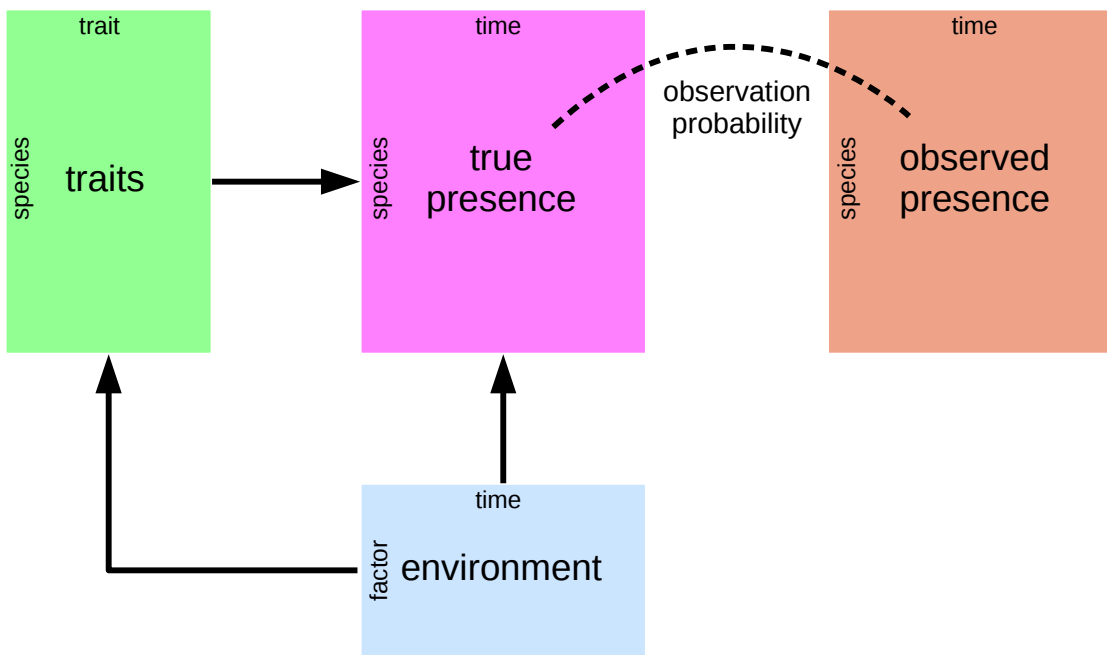


Figure 1: Conceptual diagram of the paleontological fourth corner problem. The observed presence matrix (orange) is the empirical presence/absence pattern for all species for all time points; this matrix is an incomplete observation of the “true” presence/absence pattern (purple). The estimated true presence matrix is modeled as a function of both environmental factors over time (blue) and multiple species traits (green). Additionally, the effect of environmental factors on species traits are also modeled as traits are expected to mediate the effects of a species environmental context. This diagram is based partially on material presented in Brown et al. (2014) and Warton et al. (2015).

	Time Bin							
	1	2	3	4	5	6	7	8
Observed	0	0	0	1	0	1	1	0
Certain	?	?	?	1	1	1	1	?
Potential	0	0	0	1	1	1	1	0
Potential	0	0	1	1	1	1	1	0
Potential	0	1	1	1	1	1	1	0
Potential	1	1	1	1	1	1	1	0
Potential	0	0	0	1	1	1	1	1
Potential	0	0	1	1	1	1	1	1
Potential	0	1	1	1	1	1	1	1
Potential	1	1	1	1	1	1	1	1

Figure 2: Conceptual figure of all possible occurrence histories for an observed species. The first row represents the observed presence/absence pattern for a single species at eight time points. The second row corresponds to the known aspects of the “true” occurrence history of that species. The remaining rows correspond to all possible occurrence histories that are consistent with the observed data. The process of parameter marginalization described in the text

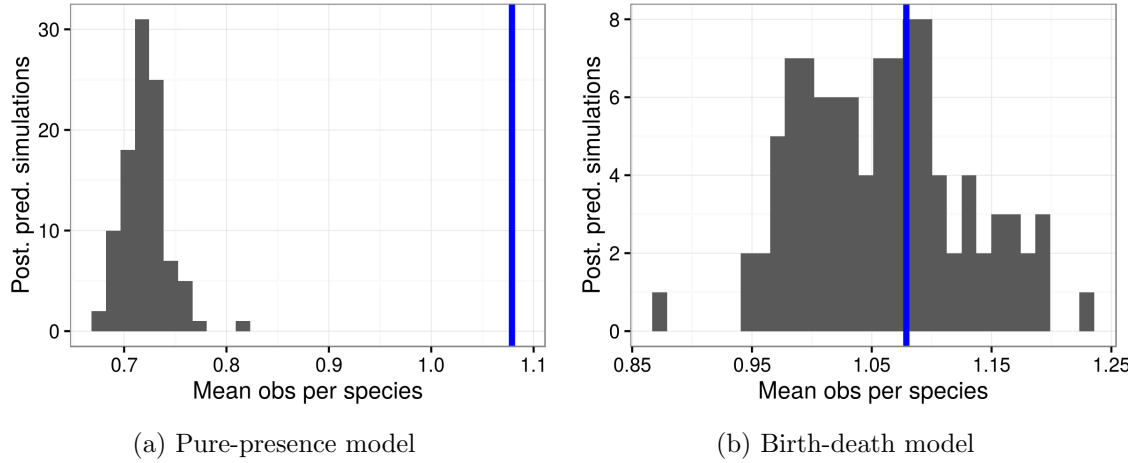


Figure 3: Comparison of the average observed number of occurrences per species (blue line) to the average number of occurrences from 100 posterior predictive datasets using the posterior estimates from the pure-presence and birth-death models.

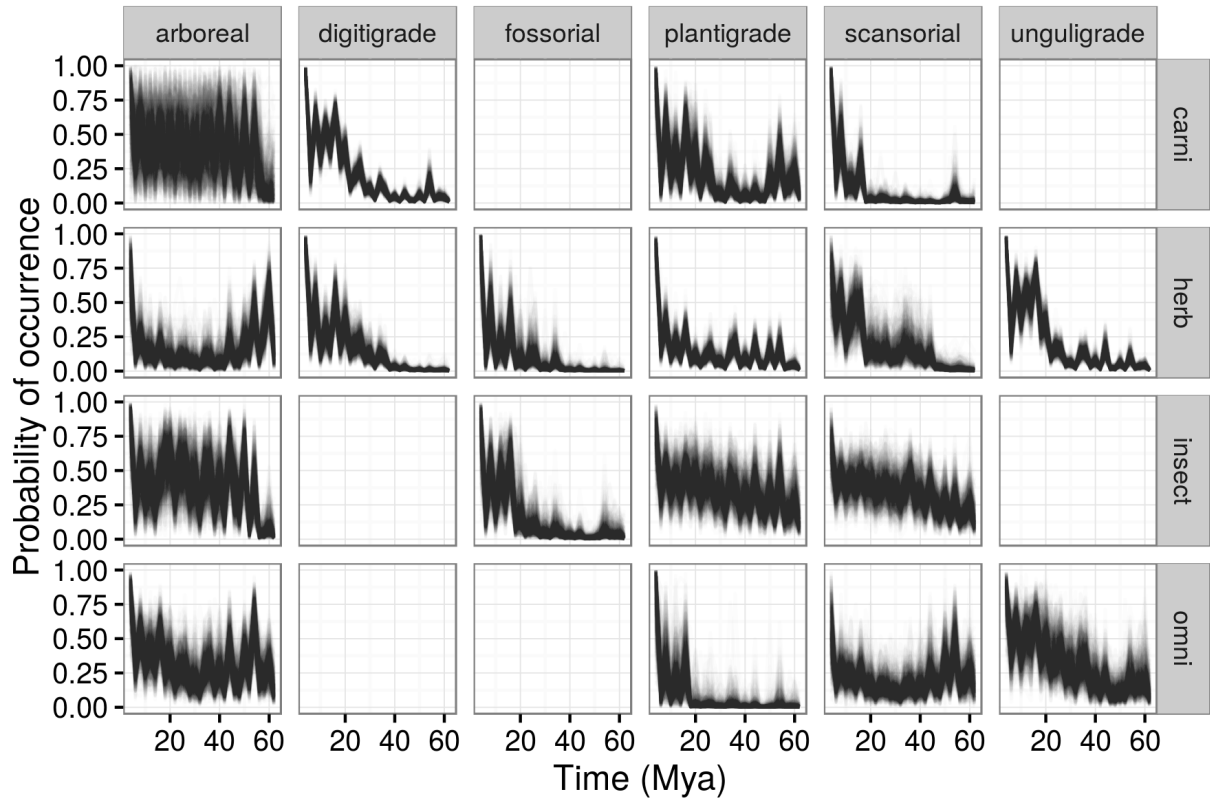


Figure 4: Probability of a mammal ecotype occurring over time as estimated from the pure-presence model. Each panel depicts 100 random samples from the model's posterior. The columns are by locomotor category and rows by dietary category; their intersections are the observed and analyzed ecotypes. Panels with no lines are ecotypes not observed in the dataset.

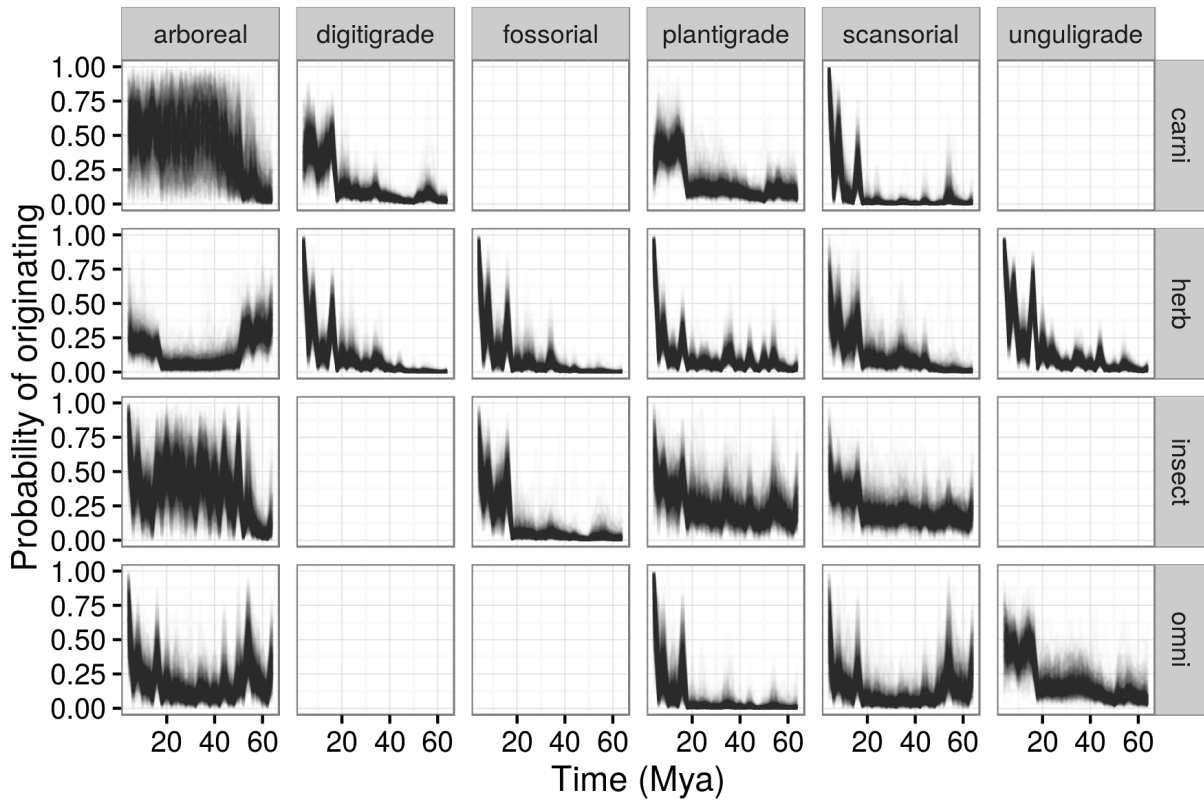


Figure 5: Probability of a mammal ecotype origination probabilities at each time point as estimated from the birth-death model. Each panel depicts 100 random samples from the model's posterior. The columns are by locomotor category and rows by dietary category; their intersections are the observed and analyzed ecotypes. Panels with no lines are ecotypes not observed in the dataset.

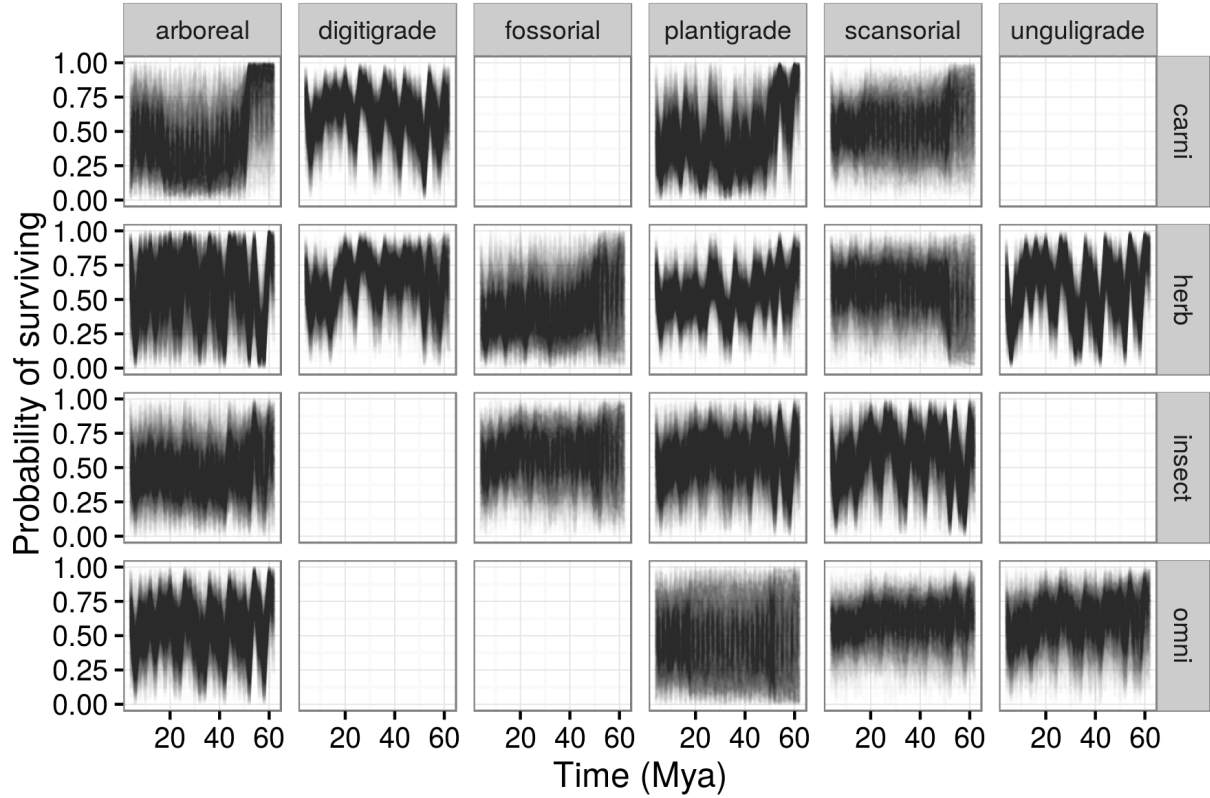


Figure 6: Probability of a mammal ecotype survival probabilities at each time point as estimated from the birth-death model. Each panel depicts 100 random samples from the model’s posterior. The columns are by locomotor category and rows by dietary category; their intersections are the observed and analyzed ecotypes. Panels with no lines are ecotypes not observed in the dataset.

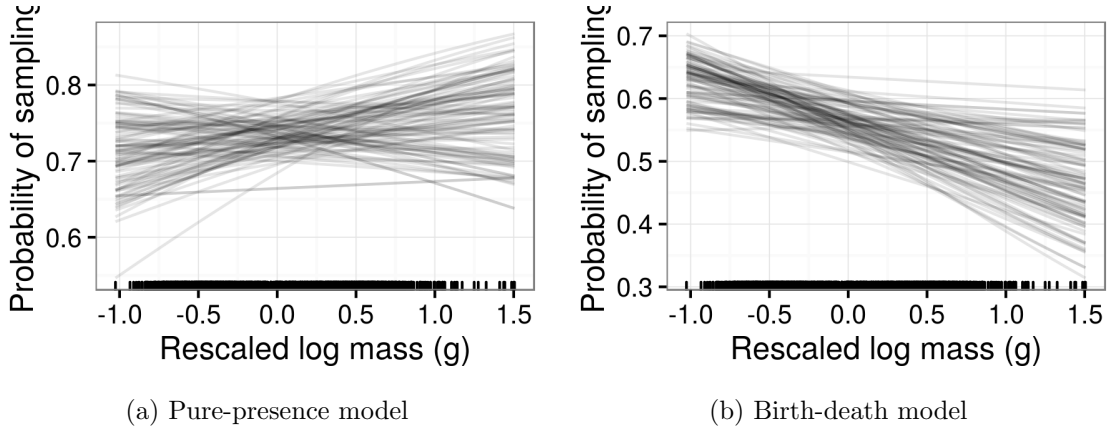


Figure 7: Estimates of the effect of species mass on probability of sampling a present species (p). Mass has been log-transformed, centered, and rescaled; this means that a mass of 0 corresponds to the mean of log-mass of all observed species and that mass is in standard deviation units. Estimates are from both the pure-presence and birth-death models.

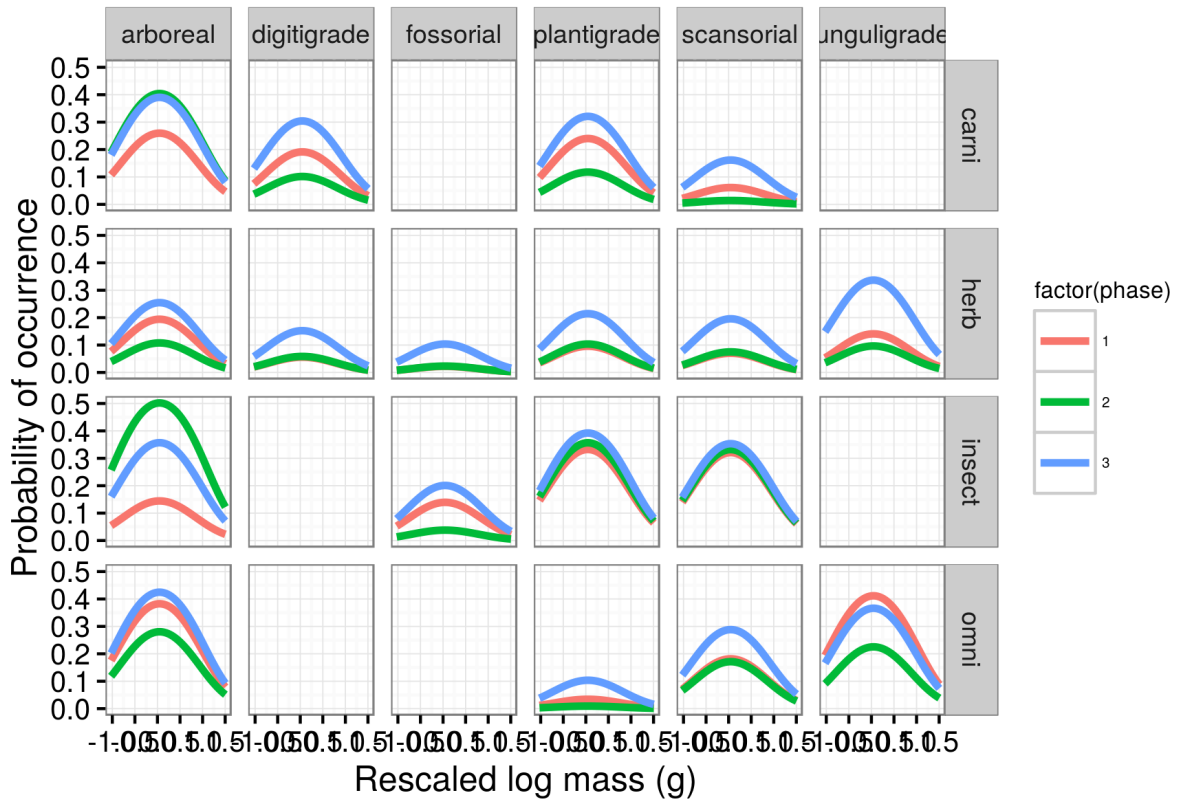


Figure 8: Mean estimate of the effect of species mass on the probability of a species occurrence for each of the three plant phases. The effect of mass is considered constant over time and that the only aspect of the model that changes with plant phase is the intercept of the relationship between mass and occurrence. The three plant phases are indicated by the color of the line. Mass has been log-transformed, centered, and rescaled; this means that a mass of 0 corresponds to the mean of log-mass of all observed species and that mass is in standard deviation units. Only the mean estimates of the effects of both mass and plant phase are plotted for clarity; these estimates are obviously made with uncertainty.

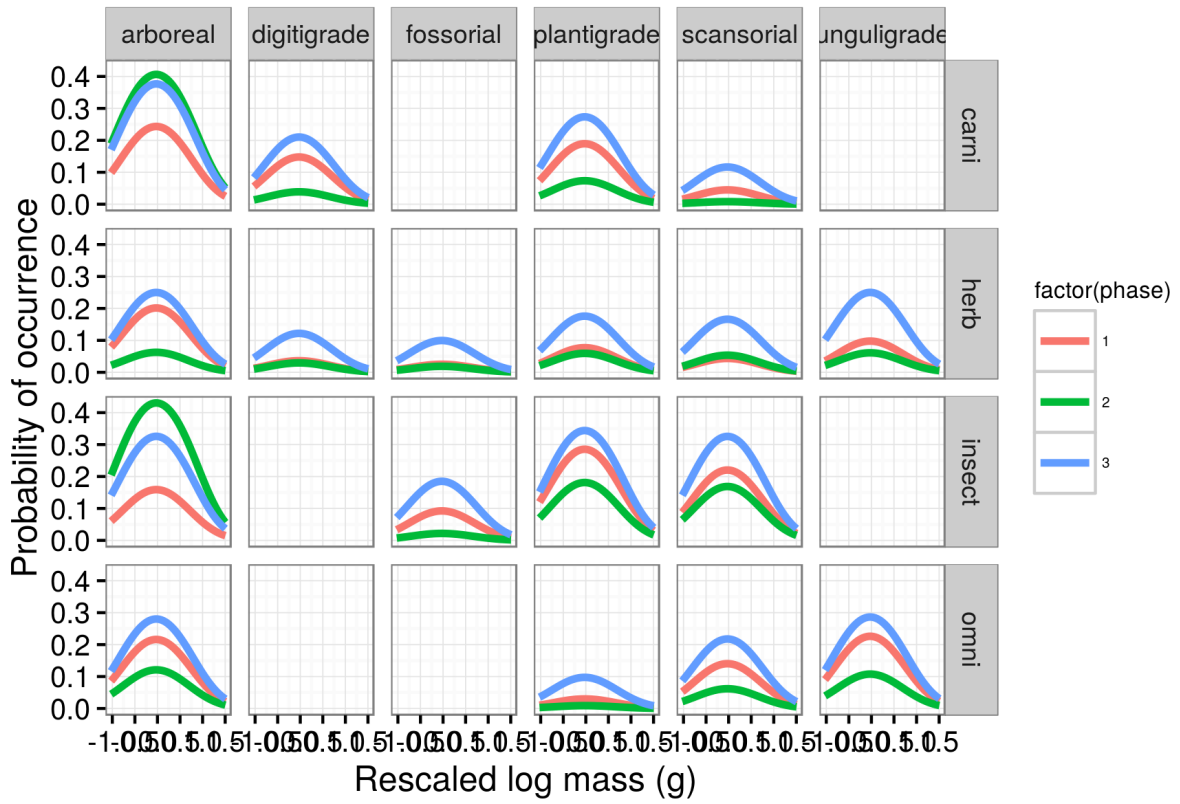


Figure 9: Mean estimate of the effect of species mass on the probability of a species originating for each of the three plant phases. The effect of mass is considered constant over time and that the only aspect of the model that changes with plant phase is the intercept of the relationship between mass and origination. The three plant phases are indicated by the color of the line. Mass has been log-transformed, centered, and rescaled; this means that a mass of 0 corresponds to the mean of log-mass of all observed species and that mass is in standard deviation units. Only the mean estimates of the effects of both mass and plant phase are plotted for clarity; these estimates are obviously made with uncertainty.

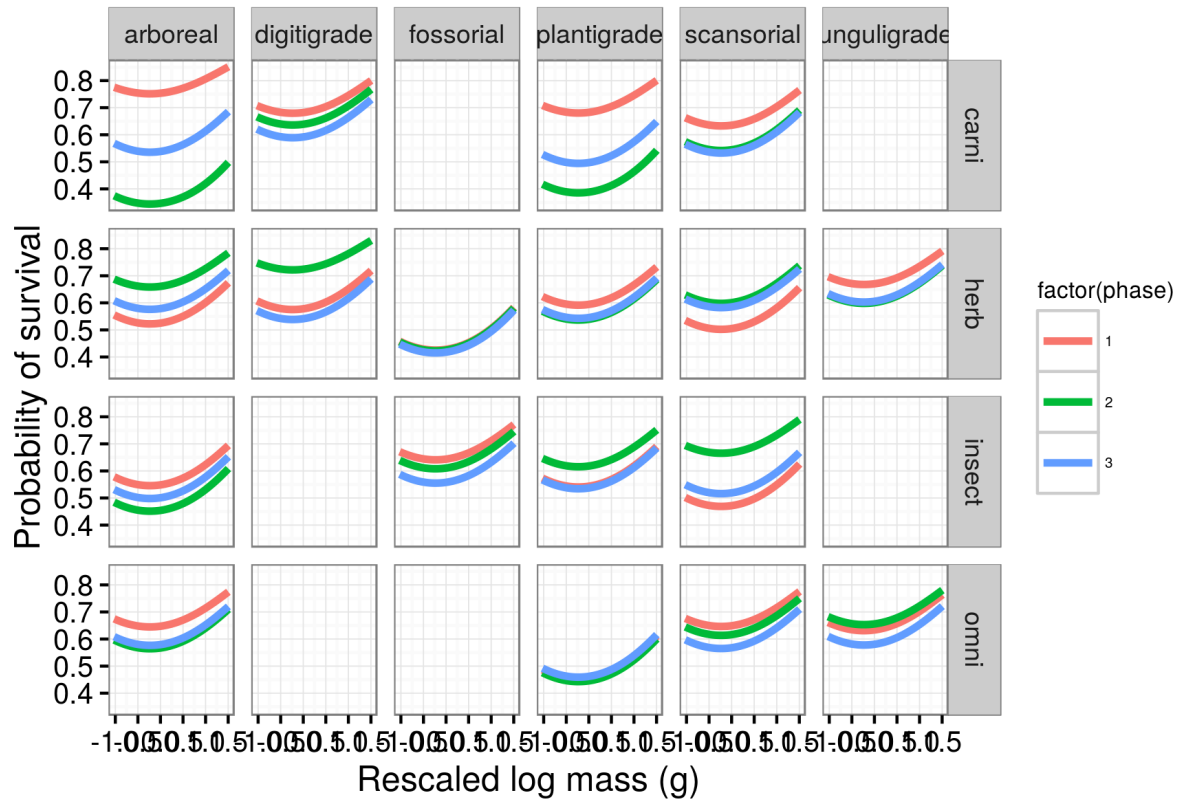


Figure 10: Mean estimate of the effect of species mass on the probability of a species survival for each of the three plant phases. The effect of mass is considered constant over time and that the only aspect of the model that changes with plant phase is the intercept of the relationship between mass and survival. The three plant phases are indicated by the color of the line. Mass has been log-transformed, centered, and rescaled; this means that a mass of 0 corresponds to the mean of log-mass of all observed species and that mass is in standard deviation units. Only the mean estimates of the effects of both mass and plant plant are plotted for clarity; these estimates are obviously made with uncertainty.

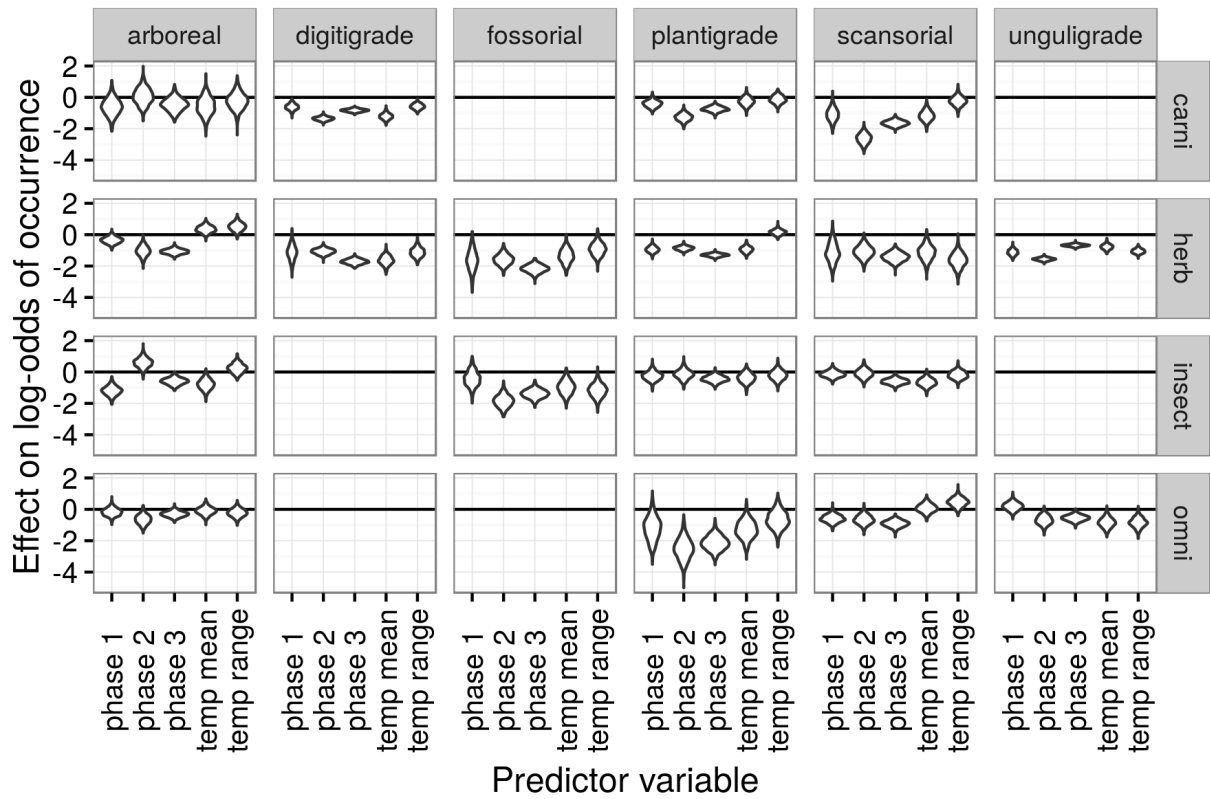


Figure 11: Estimated effects of the group-level covariates describing environmental context on log-odds of species occurrence. These estimates are from the pure-presence model.

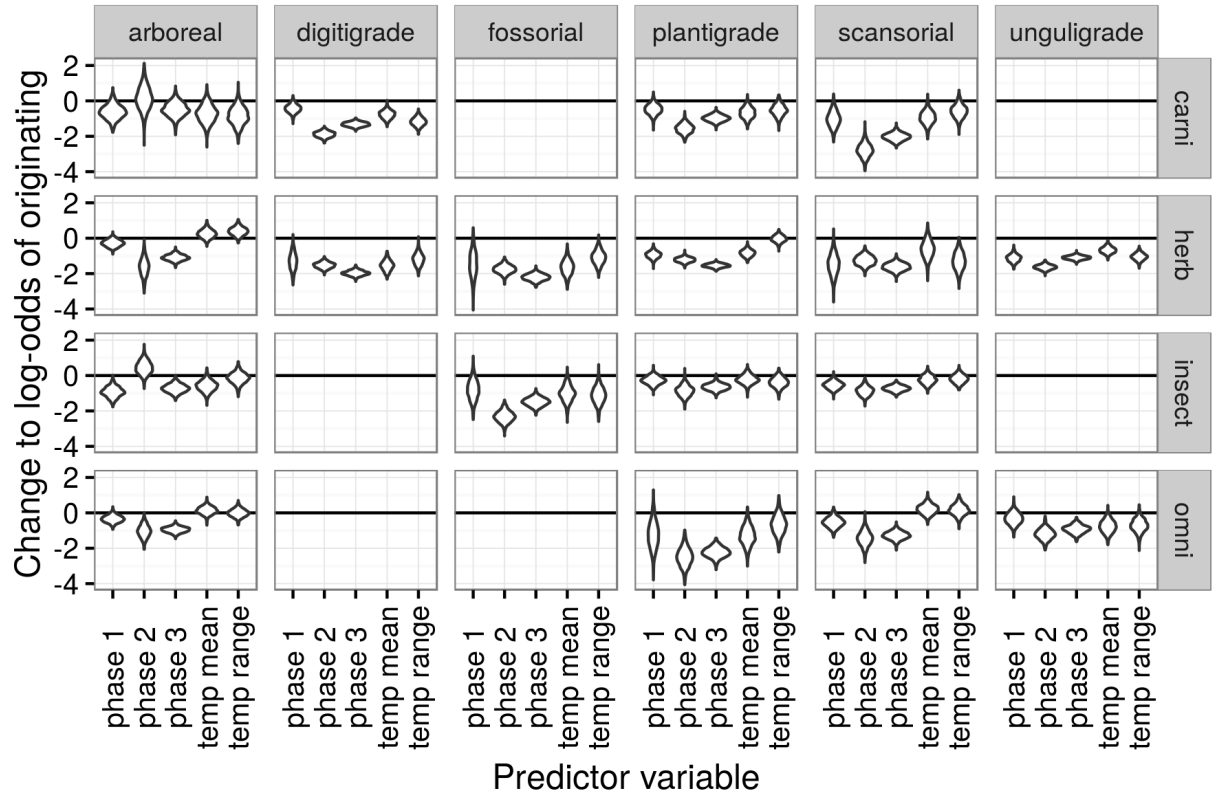


Figure 12: Estimated effects of the group-level covariates describing environmental context on log-odds of species origination. These estimates are from the birth-death model.

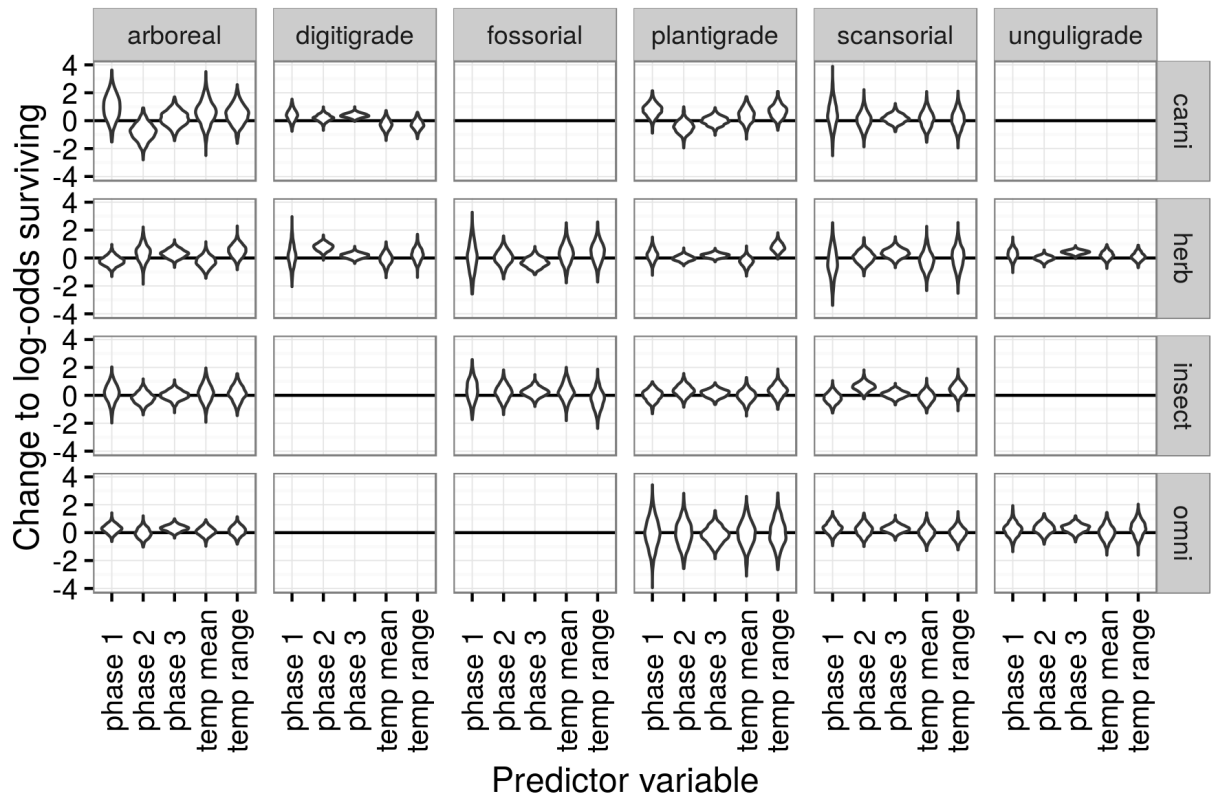


Figure 13: Estimated effects of the group-level covariates describing environmental context on log-odds of species survival. These estimates are from the birth-death model.

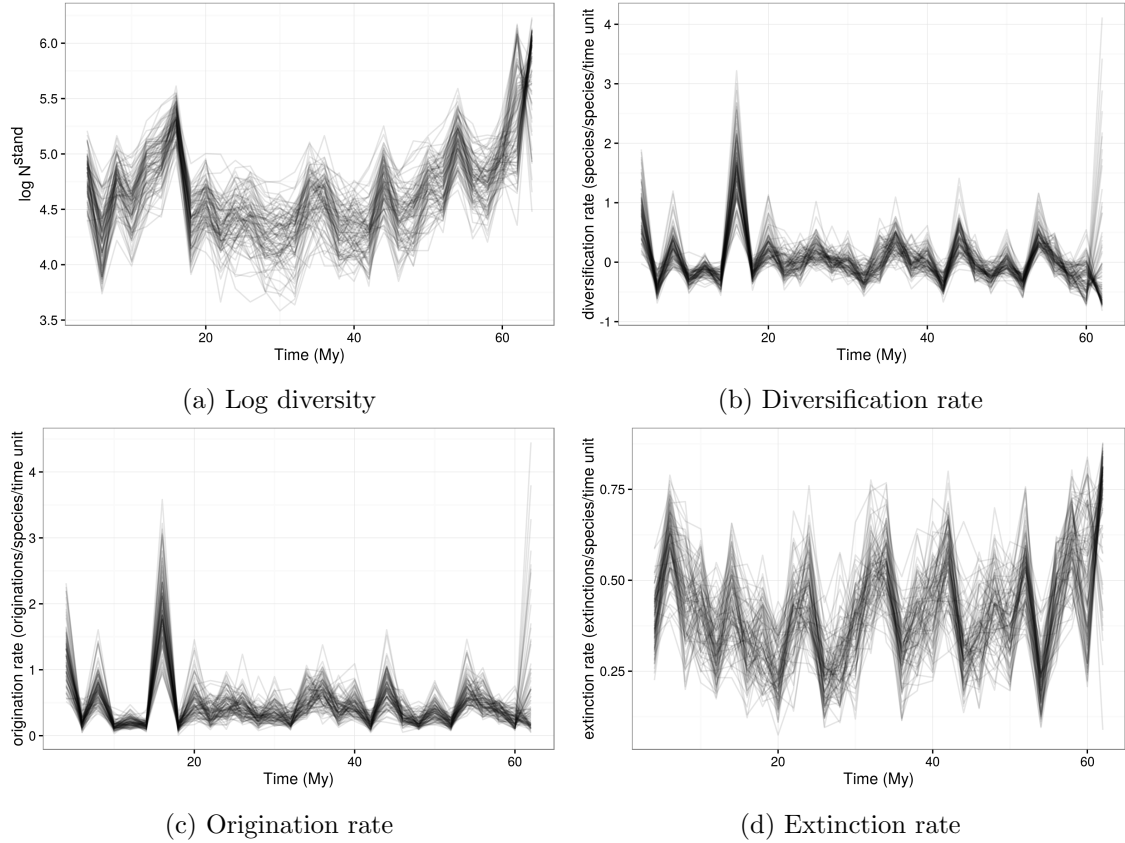


Figure 14: Posterior estimates of the time series of Cenozoic North American mammal diversity and its characteristic macroevolutionary rates; all estimates are from the birth-death model and 100 posterior draws are plotted to indicate the uncertainty in these estimates. The dramatic differences between diversity estimates at the first and second time points and the penultimate and last time points in this series are caused by well known edge effects in discrete-time birth-death models caused by $p_{-,t=1}$ and $p_{-,t=T}$ being partially unidentifiable (Royle and Dorazio, 2008); the hierarchical modeling strategy used here helps mitigate these effects but they are still present (Gelman et al., 2013; Royle and Dorazio, 2008). Diversification rate is in units of species gained per species present per time unit (2 My), origination rate is in units of species originating per species present per time unit, and extinction rate is in units of species becoming extinct per species present per time unit.

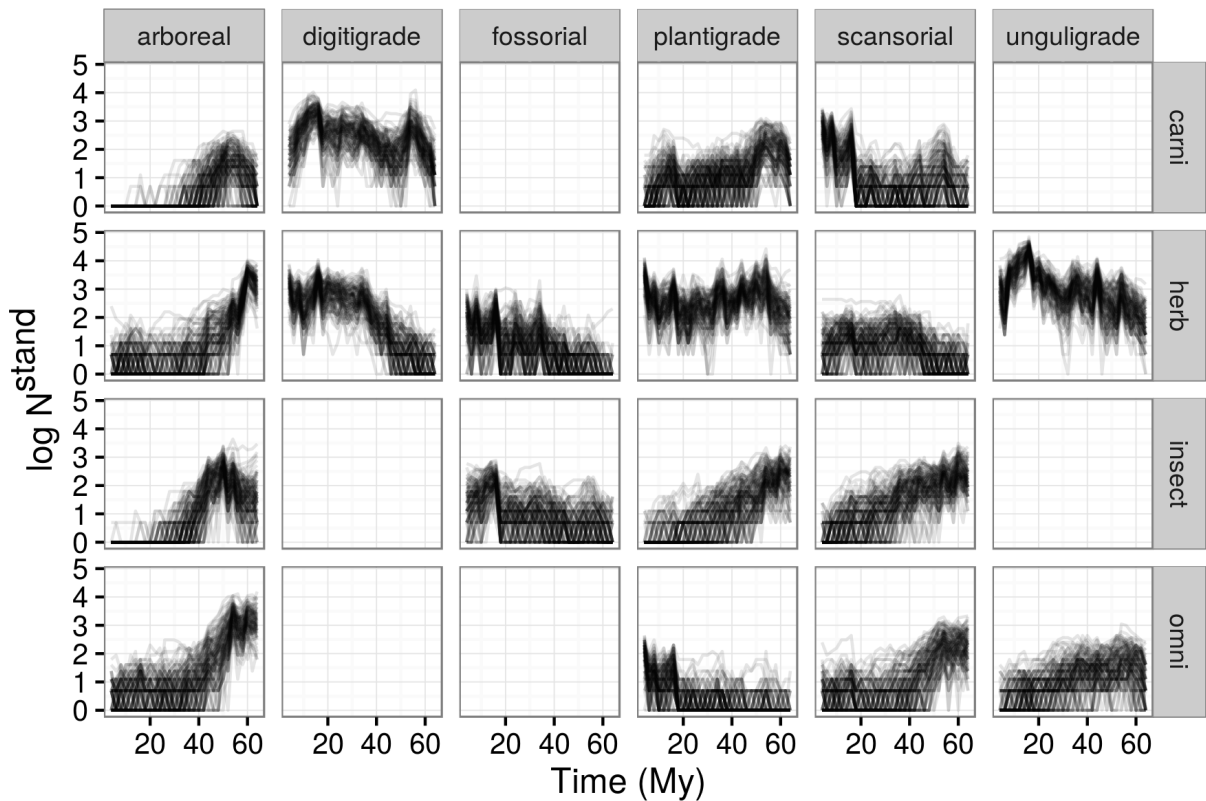


Figure 15: Posterior of standing log-diversity of North American mammals by ecotype for the Cenozoic as estimated from the birth-death model; 100 posterior draws are plotted to indicate the uncertainty in these estimates and what is technically plotted is log of diversity plus 1.